Evidence for late alluvial activity in Gale crater, Mars

John A. Grant [1], and Sharon A. Wilson [1]

[1]Center for Earth and Planetary Studies, National Air and Space Museum, Smithsonian Institution, Washington, DC, USA.

Corresponding author: John A. Grant (grantj@si.edu).

Key Points:

- Local alluvial deposits in Gale crater were likely emplaced less than 2 Ga, post-dating more widespread water-related deposits in Gale.
- Water associated with the younger alluvial deposits may be related to late-occurring diagenetic activity.
- Alluvial deposits formed when Aeolis Mons achieved its present expression, suggesting late-occurring habitable conditions within Gale.

Abstract

The occurrence of past habitable conditions in Gale crater is generally associated with lacustrine and alluvial environments present >3 Ga ago, during the Hesperian Period on Mars. However, later-occurring aqueous activity is consistent with superposition relations between some alluvial deposits and bounding materials on the crater walls, preservation of fine-scale morphology on these alluvial deposits, and their superposing crater densities. The alluvial deposits include some not previously considered, and collectively lend confidence to the interpretation that local aqueous activity persisted in Gale crater into the Amazonian, or <2 Ga ago. Our conclusions are generally in accordance with late aqueous activity inferred from geochronology data (Martin et al., 2017), in addition to late alluvial activity elsewhere. Interpreted late aqueous activity points to possible habitable settings in Gale later than previously recognized.

Plain Language Summary

Several fan-shaped deposits on the walls and floor of Gale crater formed via deposition of water transported sediment. Overall, the fan deposits are fairly well preserved, and the number of impact craters on their surfaces indicate they are much younger (~2 billion years old or less) relative to the older, more widespread water-related deposits that formed in the crater over 3 billion years ago. The late episode(s) of water-related activity in Gale crater may be associated with late-occurring chemical precipitation within and (or) cementation of older rocks within the crater, and suggests that habitable conditions persisted inside the crater later than previously thought.

1 Introduction

Gale is 154 km-diameter (D) crater located just south of the Martian dichotomy boundary at 5°S, 138°E (Fig. 1a). Gale crater formed ~3.6 to 3.8 Ga, around or after the time of the Noachian-to-Hesperian transition (Grotzinger et al., 2015; Irwin, 2013; Le Deit et al., 2012; Thomson et al., 2011). The crater interior is dominated by a ~5 km-high sedimentary mound (Aeolis Mons) that is surrounded by material flanking the walls of the crater (Aeolis Palus) (Fig. 1a). The present form of Aeolis Mons (informally known as Mt. Sharp) evolved in the Late Hesperian to Early Amazonian (Kite et al., 2013; Wray, 2013), but deposition of the mound materials may have occurred earlier (Malin & Edgett, 2000). By contrast, Aeolis Palus includes lacustrine and alluvial deposits (Grotzinger et al., 2015; Williams et al., 2013), as well as eolian and impact materials, that were mostly emplaced prior to ~3.2 Ga (Grant et al., 2014; Le Deit et al., 2013; Palucis et al., 2016).

Alluvial deposits on Aeolis Palus are variably degraded (Grant et al., 2014; Grotzinger et al., 2015), but fans in the western half of the crater (Fig. 1a) are pristine relative to most of the Aeolis Palus surface (Grant & Wilson, 2018). These fans (Fig. 1a) include some deposits associated with Peace Vallis on the northern wall of the crater (Williams et al., 2013), an unnamed deposit on the northwestern (NW) wall of the crater (Buz et al., 2017), deposits associated with Farah Vallis on the western crater wall (Palucis et al., 2016), and a “pancake delta” in the southwestern (SW) corner (Palucis et al., 2016). Each of these alluvial deposits displays and preserves superposition relationships with adjacent surfaces and preserve fine-scale

morphology that indicates they comprise some of the youngest alluvial materials within the crater.

1.1 The Peace Vallis Fan

The deposit forming the upper Peace Vallis fan (fan "1" in Fig. 1a) is separated from more degraded, pitted, and etched lower reaches by a fairly abrupt transition (Grant et al., 2014) (Fig. 1b), possibly related to later deposition of the upper fan (Grant et al., 2014) or a downslope transition to finer grain sizes (Palucis et al., 2014). Several aspects of the upper fan indicate a younger age relative to bounding deposits (Grant et al., 2014): 1) In comparison to the thicker, lower fan, the upper Peace Vallis fan deposit is only ~10-20 m thick (e.g., based on topography across and inferred beneath the fan, see Palucis et al., 2014, 2016; Grant et al., 2014) and is relatively smooth at all length scales compared to the more pitted and etched lower fan; 2) The upper fan exhibits relatively lower thermal inertia than the rougher lower fan (Anderson & Bell, 2010) and preserves a series of inverted distributary channels ~0.5 to 2.5 m high radiating from the upper fan apex (Fig. 1b); and 3) The fan is bounded by an outward facing slope and preserves a population of mostly pristine craters in contrast to many that are significantly degraded on the lower fan (Grant et al., 2014) (Fig. 1b). About 5 m of erosion is required to account for topographic inversion of putative distributary channels and is consistent with erosion predicted by the relative deficiency of craters <30 m across on the fan (for depth-to-diameter ratios of 0.1 to 0.2 (Melosh, 1989), see Grant et al., 2014). The abrupt nature of the transition between the upper and lower fan could mirror the transition to finer, more easily eroded sediments (due to a paucity of lag-forming gravel, see Palucis et al., 2014), but the transition is not marked by a significant decrease in slope (Palucis et al., 2014), pebble conglomerates occur much further down the lower fan (Williams et al., 2013), and observations of terrestrial fans indicate down-fan shifts to finer grain sizes are often not abrupt (Stock, 2013; Stock et al., 2008).

The relationship between the upper fan deposit and the largest crater visible on the upper fan (~750 m in diameter, Fig. 1b) further supports a relatively young age for the upper alluvium. The crater displays an asymmetric rim that is narrow and of lesser relief (relative to crater depth) on the uphill side rather than on the downhill side, which is consistent with fan material embaying the crater from the uphill direction (Grant et al., 2014). Moreover, a segment of an inverted channel occurring about one diameter from the southwest rim (Grant et al., 2014) is not buried by ejecta (Fig. 1b). The expression of the crater and nearby fan surface in THEMIS nighttime infrared (IR) data (Christensen et al., 2004) indicates that the inverted channel segment is likely part of a larger distributary that is deflected around the west side of the crater (Fig. 1c), thereby suggesting relief associated with the crater was likely present when the channel incised. Finally, concentric fractures surrounding the crater could relate to primary impact features (Palucis et al., 2016), but alternatively may reflect differential compaction of younger embaying alluvium that thins towards the crater rim.

1.2 The Northwestern Fan Deposit

A deposit on the northwestern wall of the crater (fan "2" in Fig. 1a) shares many of the attributes of the upper Peace Vallis fan. Buz et al. (2017) described the deposit as a dark cliff forming unit that is smooth at all length scales, ~20 m thick, and expresses several inverted channels radiating downslope from the crater wall that are of a similar scale to those observed on Peace Vallis (Fig. 1d). The deposit is spectrally bland, is bounded by outward facing slopes and

caps local Aeolis Palus stratigraphy, and may post-date water-rich periods in Gale (Buz et al., 2017). Part of the western portion of the deposit appears to be mantled by ejecta from the ~6 km-diameter Slangpos crater to the west (Fig. 1a). Although Buz et al. (2017) interpreted the deposit as a fluvially facilitated mass wasting deposit, or perhaps airfall deposit, we favor a fluvial interpretation with perhaps some contributions from mass wasting for several reasons. First, the broad similarity with Peace Vallis morphologies, local occurrence, abrupt boundary of the deposit with adjacent Aeolis Palus materials, radiating and inverted channels, and confinement to local lows (e.g., rather than superposing local craters) argues for an alluvial or fluvial origin with the inverted channels recording the occurrence of past distributaries (Fig. 1d). These same attributes are not consistent with an airfall origin where associated deposits would be expected to mantle variable relief and lack associated channels. Moreover, the preservation of small inverted channels is inconsistent with occurrence as a degraded remnant of a once larger airfall deposit. Contributions from mud or debris flows are possible, but the absence of a head scarp, the low profile of the deposit, and absence of recognizable transverse ridges or cracks, radial cracks, or toes along the terminus (e.g., Easterbrook, 1993; Ritter et al., 1995) argue against origin as a dry rock or debris slide.

1.3 Farah Vallis Fans

A series of deposits associated with Farah Vallis on the SW wall of Gale (e.g., Ehlmann & Buz, 2014) also appear to be very young (deposits "3," "4," and "5" in Fig. 1a). Upper surfaces are characterized by several well-preserved but abandoned channel segments that are truncated by more deeply incised segments (Fig. 1e). Some of the abandoned segments terminate at downhill facing scarps that may record locations of temporary stability during a period when headward incision eventually resulted in a single discharge channel that debouched water and sediment across an alluvial fan lower on the crater wall/floor (Fig. 1f). Dunes encroaching from the north (Fig. 1f) make it difficult to map the full extent of the fan, but much like the deposits associated with Peace Vallis and along the NW wall of the crater, the fan otherwise embays other surfaces in the crater. The fan preserves a series of distributaries radiating from the terminus of the incised segment of Farah Vallis (Fig. 1f), including one near the center of the deposit that averages 80 m wide and extends for approximately 5 km (Palucis et al., 2016).

1.4 Southwestern Fan Deposit ("pancake delta")

A fourth deposit located east of Farah Vallis (fan "6" in Fig. 1a), may also be associated with discharge from Farah Vallis, and is probably a classic Gilbert-type delta that formed into standing water (e.g., with distinctive topset, foreset, and bottomset beds that formed by accumulation of relatively coarser as opposed to muddier sediments, see Palucis et al., 2016) (Fig. 1g). Like the other deposits discussed herein, the deposit embays adjacent materials (Figs. 1g and 1h). As summarized from Palucis et al. (2016), the deposit (dubbed the "pancake delta") preserves slopes that decrease distally from approximately two to one degree, and then abruptly transitions to an outward facing and largely unincised slope of close to seven degrees along a constant elevation. The deposit is on order of 100 m thick and marked by numerous small craters, many of which are partially sediment filled and (or) show eroded rims (Palucis et al., 2016) (Fig. 1g). The pancake delta does not preserve extensive distributaries or other channels, is locally covered by eolian materials, and may be somewhat more degraded than the other deposits discussed. Nevertheless, there is the faint expression of features radiating from near the western

apex of the deposit that are likely segments of distributaries (Fig. 1h), thereby highlighting the overall well-preserved nature of the deposit.

All of the alluvial deposits clearly superpose adjacent Aeolis Palus materials with the exception of some limited eolian materials encroaching on the Farah Vallis fans and the pancake delta. Each of the deposits also preserves fine-scale, and in most cases – with the exception of the pancake delta – meter-scale morphologies associated with their formation that highlights their pristine state. Finally, their stratal position and preservation require that discharge associated with their emplacement occurred very late in the geomorphic evolution of the crater and was perhaps the last non-impact or eolian event that took place. Nevertheless, uncertainty remains regarding whether their emplacement closely followed major geomorphic events in the crater (e.g., Grant et al., 2014; Grotzinger et al., 2015), or if they formed considerably later, perhaps associated with late fluid flow and formation of secondary materials in some rocks in the crater (Martin et al., 2017). This study compiles the statistics from the population of craters on the alluvial deposits to provide further constraints on the timing of their formation.

2 Background and Motivation

Crater statistics constrain the timing of geomorphic activity in Gale crater, including the formation of Aeolis Palus, and place components of the landscape in a broader geologic framework (e.g., Buz et al., 2017; Grant et al., 2014, Grotzinger et al., 2015; Palucis et al., 2016). Prior attempts to determine the age of the Peace Vallis fan using crater statistics suggested it was young, perhaps even Amazonian in age (Grant et al., 2014). Those counts, however, were based on very small counting areas that may not capture the natural variability in crater density and (or) larger more widely spaced craters (e.g., Palucis & Dietrich, 2014; Thomson & Fassett, 2015; Warner et al., 2015), and were thus inconclusive (Grant et al., 2014). Here, we combine the areas of all deposits discussed herein to achieve a larger counting area, an approach justified by their common stratal position, pristine state, and formation process. We also take care to establish the stratigraphic position of contributing craters (e.g., Barlow, 2015; Grant et al., 2014) after the example described for evaluating the relative age of the ~750 m diameter crater associated with the upper Peace Vallis fan. The result is high confidence in contributing craters and a total count area of 429 km^2. By comparison, counts completed on Aeolis Palus, which range in area from under 300 km^2 to 1000s of km^2, all yield similar interpreted ages that indicate the surface was largely in place by ~3.2 Ga (e.g. Grant et al., 2014; Grotzinger et al., 2015; Le Deit et al., 2013; Palucis et al., 2016). Consistent interpretation of ages for Aeolis Palus made from counts covering a range of areas, including some smaller than the combined area covered by the four younger alluvial deposits considered here, provides confidence that the combined counting area of the fans is sufficient to yield a reliable interpreted emplacement age.

3 Methods

Crater statistics were compiled in ArcGIS using data from the Context Camera (CTX) (Malin et al., 2007) on the Mars Reconnaissance Orbiter and CraterTools software (Kneissl et al., 2011). The 6 m/pixel scale of CTX data enabled confident definition of craters >20 m in diameter and counts excluded obvious secondary clusters and western portions of the NW deposit that may be overlain by ejecta from Slangpos crater (Fig. 1a). Counts were made using individual CTX images to minimize variable lighting and image quality effects (see Fig. S1). To further reduce effects of image resolution and even small amounts of erosion, craters smaller than 100 m in

diameter were not included in the interpretation. The derived age for the combined fan area with craters from all of the alluvial deposits (Fig. 1a) was made from the segment (0.17 to 0.70 km in diameter) of the plot best matching the expected production population using "pseudo-log" binned reverse cumulative histograms and Craterstats2 software (Michael & Neukum, 2010). Absolute ages are based on the chronology function of Hartmann & Neukum (2001), and production functions from both Ivanov (2001) and Hartmann (2005), though the Ivanov (2001) ages are emphasized for ease of comparison with prior results (e.g., Grant et al., 2014). An interpreted age was also derived from the incremental plots using the variable diameter bin-size method of Hartmann (2005). Although the relative timing of events can be constrained with confidence using crater statistics, interpretation of the absolute ages derived for the alluvial deposits is model dependent on the flux rate of impactors at Mars and incorporates uncertainty of around a factor of two (Hartmann & Neukum, 2001). We acknowledge this general level of uncertainty in absolute age interpretations.

4 Results

Cumulative statistics for the combined area of the alluvial deposits (Fig. 2) are very close to the expected production population (Ivanov, 2001) for the 143 craters at diameters over 170 m up to the largest crater of 667 m, but are relatively deficient in smaller craters due to limited ongoing erosion and incomplete inclusion (Fig. 2a). Importantly, comparison between statistics for Aeolis Palus and the count for all of the fans shows the density of craters on the fans is less at all diameters used in interpretation of ages (Fig. 2a). The diameter range matching the production population on the fans yields a modeled absolute age of ~1.3 Ga and ~1.8 Ga using the production function from Ivanov (2001) and Hartmann (2005), respectively, and is significantly younger than the ~3.3 Ga modeled age for Aeolis Palus using craters larger than 500 m in diameter (both the Ivanov (2001) and Hartmann (2005) production functions yield similar results, see also Grant et al., 2014). Incremental statistics for the fans are similar, though there is a possible excess of several larger craters relative to the expected production population (Fig. 2b). Age interpretations made for the fans using just the 48 craters larger than 230 m in diameter yield an age of ~1.5 Ga and ~1.9 Ga using the production function from Ivanov (2001) and Hartmann (2005), respectively, and may better fit the incremental plot. Nevertheless, the difference in interpreted ages from the two plots may relate to differences in the production function and position of hypothesized isochrones (Carr, 2006; Hartmann, 2005). With the understanding that interpreted ages represent the minimum age of the fan surfaces (end of geomorphic activity associated with their emplacement), we emphasize the slightly younger values derived from the cumulative statistics.

We excluded craters from the count that were identified as being mantled by the fan deposits, including the ~750 m-diameter crater on the upper Peace Vallis fan (Figs. 1b and 1c). In order to calibrate the sensitivity of the results to exclusion of one or more of these large craters, inclusion of the ~750 m-diameter crater shifts the interpreted age older by less than 0.1 Ga. This supports the fundamental interpretation that the fans (in Fig. 1a) are substantially younger than Aeolis Palus, regardless of the potential misclassification and (or) inclusion of several craters.

5 Discussion

Crater statistics for the combined area of the fan deposits yield interpreted ages that are considerably younger than the age derived for the broader Aeolis Palus, consistent with the

stratal position and fine-scale of preserved morphology of the fans. Data for fan deposits strongly suggest an episode of fluvial activity that shaped local surfaces in Gale around 1.3 Ga, significantly later than cessation of activity associated with formation of Aeolis Palus at ~3.3 Ga. Ages interpreted using fewer craters at larger diameters may better fit the incremental plot, but still result in fan ages of 1.5 Ga and all reasonable derived ages are much less than the age of Aeolis Palus. Nevertheless, the limited extent and volume of the alluvial deposits are most consistent with a limited total volume and duration of water activity at this late stage relative to the earlier lacustrine environment within Gale (Grotzinger et al., 2015).

Within the range and uncertainty of absolute age interpretations for the fan deposits, the timing of a late period of water-driven activity in Gale may be consistent with the results of K-Ar dating of a jarosite-bearing mudstone in Gale (Martin et al., 2017). That work yields a formation age of secondary materials <3.0 Ga (2.12 +/-0.36) consistent with late post-depositional fluid flow that emplaced diagenetic materials in the subsurface (Martin et al., 2017). Moreover, the sample used for K-Ar dating was taken downslope of the apparently younger, more pristine upper Peace Vallis fan. The more degraded appearance of the lower fan suggests that runoff responsible for shaping the upper fan did not reach the lower fan, but instead may have infiltrated near the lower margin of the upper fan. Infiltration of runoff on the upper fan could then have sourced the groundwater that likely contributing to diagenetic processes in the subsurface at lower elevations (Grotzinger et al., 2014, 2015; Martin et al., 2017).

The timing of late fan activity also approximately correlates with establishment of the current form of Aeolis Mons in the Amazonian (Kite et al., 2013; Wray, 2013). Limited, possible incision of Aeolis Mons and candidate associated depositional forms (e.g., Gediz Vallis ridge and the Greenheugh pediment on the north side, and the "Grand Canyon" on the southwest side (Bryk et al., 2019; Hughes et al., 2019)) implies that late alluvial activity was not limited to fans described herein, and was likely associated with a spike in broader geomorphic activity. Moreover, assessment of watersheds contributing to Gale crater (Ehlmann & Buz, 2014) potentially extend the source of late water well outside of the crater rim. Alluvial fans elsewhere on Mars also record a late period of aqueous activity (Grant & Wilson, 2011, 2012; Morgan et al., 2013), suggesting that potentially habitable environments at the surface, and possibly subsurface, persisted at least locally within Gale (and elsewhere) into the Amazonian.

Acknowledgements

We thank the Jet Propulsion Laboratory, University of Arizona, Ball Aerospace, Malin Space Science Systems, and Lockheed Martin that built and operate the Curiosity rover, HiRISE and CTX cameras, and the Mars Reconnaissance Orbiter. We appreciate constructive reviews by Aileen Yingst and David Crown that improved the manuscript. This work was supported by JPL/NASA subcontract 1546619 awarded to J. A. Grant. The data used are listed in the figures and (or) repository at http://airandspace.si.edu/CEPSData.

References

Anderson, R. B., and J. F. Bell III (2010), Geologic mapping and characterization of Gale crater and implications for its potential as a Mars Science Laboratory landing site, *Mars*, *5*, 76-128, doi:10.1555/mars.2010.0004.

Barlow, N. (2015), Characteristics of impact craters in the northern hemisphere of Mars. In Large Meteorite Impacts and Planetary Evolution V (Vol. 518, pp. 31-63). (Special Paper of the

Geological Society of America; Vol. 518), Geological Society of America, https://doi.org/10.1130/2015.25183.
Bryk, A. B., W. E. Dietrich, M. P. Lamb, J. P. Grotzinger, A. R. Vasavada, K. M. Stack, R. Arvidson, C. Fedo, K. Bennett, V. K. Fox, S. Gupta, R. C. Wiens, R. M. E. Williams (2019), In Curiosity's path: The geomorphology and stratigraphy of the Greenheugh pediment and Gediz vallis ridge in Gale crater, *LPSC L*, 2263.
Buz, J., B. L. Ehlmann, L. Pan, and J. P. Grotzinger (2017), Mineralogy and stratigraphy of the Gale crater rim, wall, and floor units, *J. Geophys. Res. Planets*, *122*, 1090–1118, doi:10.1002/2016JE005163.
Calef III, F. J., and T. Parker (2016), MSL Gale Merged Orthophoto Mosaic, Publisher: PDS Annex, U.S. Geological Survey, URL: http://bit.ly/MSL_Basemap.
Carr, M. H. (2006), *The Surface of Mars*, Cambridge Univ. Press, Cambridge, UK, 307p.
Christensen, P. R., et al. (2004), The Thermal Emission Imaging System (THEMIS) for the Mars 2001 Odyssey Mission, *Space Sci. Rev.*, 110 (1 – 2), 85 – 130, doi:10.1023/B:SPAC.0000021008.16305.94
Easterbrook, D. J. (1993), *Surface Processes and Landforms*, Macmillan Publishing Company, New York, NY, 520 pp.
Ehlmann, B. L., and Buz, J. (2014), Mineralogy and fluvial history of the watersheds of Gale, Knobel, and Sharp craters: A regional context for the Mars Science Laboratory Curiosity's exploration, *Geophys. Res. Letts.*, *42*, 264-273, doi:10.1002/2014GL062553.
Grant, J. A., and S. A. Wilson (2011), Late alluvial fan formation in southern Margaritifer Terra, Mars, *Geophys. Res. Letts*., *38*, L08201, doi:10.1029/2011GL046844.
Grant, J. A., and S. A. Wilson (2012), A possible synoptic source of water for alluvial fan formation in southern Margaritifer Terra, Mars, *Planet. Space Sci.*, *72*, 44-52, 10.1016/j.pss.2012.05.020.
Grant, J. A., and S. A. Wilson (2018), Possible geomorphic and crater density evidence for late aqueous activity in Gale crater, LPSC XLIX, Abstract 2102.
Grant, J. A., S. A. Wilson, N. Mangold, F. Calef III, and J. P. Grotzinger (2014), The timing of alluvial activity in Gale crater, Mars, *Geophys. Res. Lett*., *41*, 1142–1148, doi:10.1002/2013GL058909.
Grotzinger, J. P., et al. (2014), A habitable fluvio-lacustrine environment at Yellowknife Bay, Gale Crater, Mars, *Science*, DOI: 10.1126/science.1242777.
Grotzinger, J. P., et al. (2015), Deposition, exhumation, and paleoclimatology of an ancient lake deposit, Gale crater, Mars, *Science*, *350*, DOI: 10.1126/science.aac7575.
Hartmann, W. K. (1984), Does crater 'saturation equilibrium' occur in the solar system?
Icarus, 60, 56-74, 10.1016/0019-1035(84)90138-6.
Hartmann, W. K. (2005), Martian cratering 8: Isochron refinement and the chronology of Mars, *Icarus*, *174*, 294-320.
Hartmann, W. K., and G. Neukum (2001), Cratering chronology and the evolution of Mars, *Space Science Reviews*, *96*, 165–194.
Hughes, M. N., R. E. Arvidson, A. B. Bryk, W. E. Dietrich, M. P. Lamb, and J. G. Catalano (2019), Debris deposits within the upper Gediz vallis and Grand Canyon of Gale crater, *LPSC L*, 3196.
Irwin, R. P. (2013), Testing links between impacts and fluvial erosion on post-Noachian Mars, *LPSC XLIV*, 2958.

Ivanov, B. A. (2001), Mars/Moon cratering ratio estimates, *Space Science Review*, *96*, 87–104.
Kite, E. S., K. W. Lewis, M. P. Lamb, C. E. Newman, and M. I. Richardson (2013), Growth and form of the mound in Gale Crater, Mars: Slope wind enhanced erosion and transport, *Geology*, doi:10.1130/G33909.1
Kneissl, T., S. van Gasselt, and G. Neukum (2011), Map-projection-independent crater size-frequency determination in GIS environments—New software tool for ArcGIS, *Planet. Space Sci.*, *59*, 1243-1254, doi:10.1016/j.pss.2010.03.015.
Le Deit, L., E. Hauber, F. Fueten, N. Mangold, M. Pondrelli, A. Rossi, and R. Jaumann (2012), Model age of Gale crater and origin of its layered deposits, *3rd Int. Early Mars*, 7045.
Le Deit, L., E. Hauber, F. Fueten, M. Pondrelli, A. P. Rossi, and R. Jaumann (2013), Sequence of infilling events in Gale Crater, Mars: Results from morphology, stratigraphy, and mineralogy, *J. Geophys. Res. Planets*, 118, 2439–2473,doi:10.1002/2012JE004322.
Malin, M. C., and K. S. Edgett (2000), Sedimentary rocks of early Mars, *Science*, *290*, 1927-1937, doi:10.1126/science.290.5498.
Malin, M. C., et al. (2007), Context Camera Investigation on board the Mars Reconnaissance Orbiter, *J. Geophys. Res.*, *112*, E06S04, doi:10.1029/2006JE002808.
Martin, P. E., K. A. Farley, M. B. Baker, C. A. Malespin, S. P. Schwenzer, B. A. Cohen, and R. NavarroGonzález, (2017), A two-step K-Ar experiment on Mars: Dating the diagenetic formation of jarosite from Amazonian groundwaters. *J. Geophys. Research: Planets*, *122*, 2803–2818. https://doi.org/10.1002/2017JE005445.
Melosh, H. J. (1989), *Impact Cratering*, 245 pp., Oxford University Press, New York.
Michael, G. G., and G. Neukum (2010), Planetary surface dating from crater size-frequency distribution measurements: Partial resurfacing events and statistical age uncertainty, *Earth and Planet. Sci. Letts.*, doi:10.1016/j.epsl.2009.12.041.
Morgan, A. M., A. D. Howard, D. E. J. Hobley, J. M. Moore, W. E. Dietrich, R. M. E. Williams, D. M. Burr, J. A. Grant, S. A. Wilson, and Y. Matsubara (2013), Sedimentology and climatic environment of alluvial fans in the martian Saheki crater and a comparison with terrestrial fans in the Atacama Desert, *Icarus*, *229*, 131-156.
Palucis, M. C., and W. E. Dietrich (2014), How small is too small? A simple model for assessing uncertainties of individual crater age measurements for martian surfaces, *LPSC* XLV, 2353.
Palucis M. C, W. E. Dietrich, A. G. Hayes R. M. E. Williams, D. Sumner, N. Mangold, N. Horton, S. Gupta, F. Calef, and C. Hardgrove (2014), Origin and Evolution of the Peace Vallis fan system that drains to the Curiosity landing site, J. *Geophys. Res., Planets, 119(4)*, 705-728, doi: 10.1002/2013JE004583.
Palucis, M. C., A. G. Hayes, R. M. E. Williams, D. Sumner, N. Mangold, N. Horton, T. Parker, K. Lewis, and W. E. Dietrich (2016), Sequence and relative timing of large lakes in Gale Crater (Mars) after the formation of Mt. Sharp, *JGR –Planets*, doi: 10.1002/2015JE004905.
Ritter, D. F., R. C. Kochel, and J. R. Miller (1995), *Process Geomorphology*, Wm. C. Brown, Co., Dubuque, Iowa, 540pp.
Stock, J. D. (2013), Waters divided: A history of alluvial fan research and a view of its future, in *Treatise on Geomorphology*, vol. 9, edited by J. Shroder and E. Wohl, pp. 413-458, Academic Press, San Diego, Calif.
Stock, J. D., K. M. Schmidt, and D. M. Miller (2008), Controls on alluvial fan long profiles, Geol. Soc. Am. Bull., 120(5–6), 619–640, doi:10.1130/B26208.1.

Thomson, B. J., and C. I. Fassett (2015), Issues with counting craters on small areas: Fool me twice, LPSC XLVI, 2665.
Thomson, B. J., N. T. Bridges, R. Milliken, A. Baldridge, S. J. Hook, J. K. Crowley, G. M. Marion, C. R. de Souza Filho, A. J. Brown, and C. M. Weitz (2011), Constraints on the origin and evolution of the layered mound in Gale Crater, Mars using Mars Reconnaissance Orbiter data, *Icarus*, *214*, 413–432, doi:10.1016/j.icarus.2011.05.002.
Warner, N. H., S. Gupta, F. Calef, P. Grindrod, N. Boll, and K. Goddard (2015), Minimum effective area for high resolution crater counting of Martian terrains, *Icarus*, *245*, 198–240, doi:10.1016/j.icarus.2014.09.024.
Williams, R. M. E., et al. (2013), Martian fluvial conglomerates at Gale crater, *Science*, *340*, 1068-1072, doi: 10.1126/science.1237317.
Wray, J. J. (2013), Gale crater: the Mars Science Laboratory/Curiosity Rover Landing Site, *Int. J. Astrobiol*. *12*, 25-38, doi: http://dx.doi.org/10.1017/S1473550412000328.

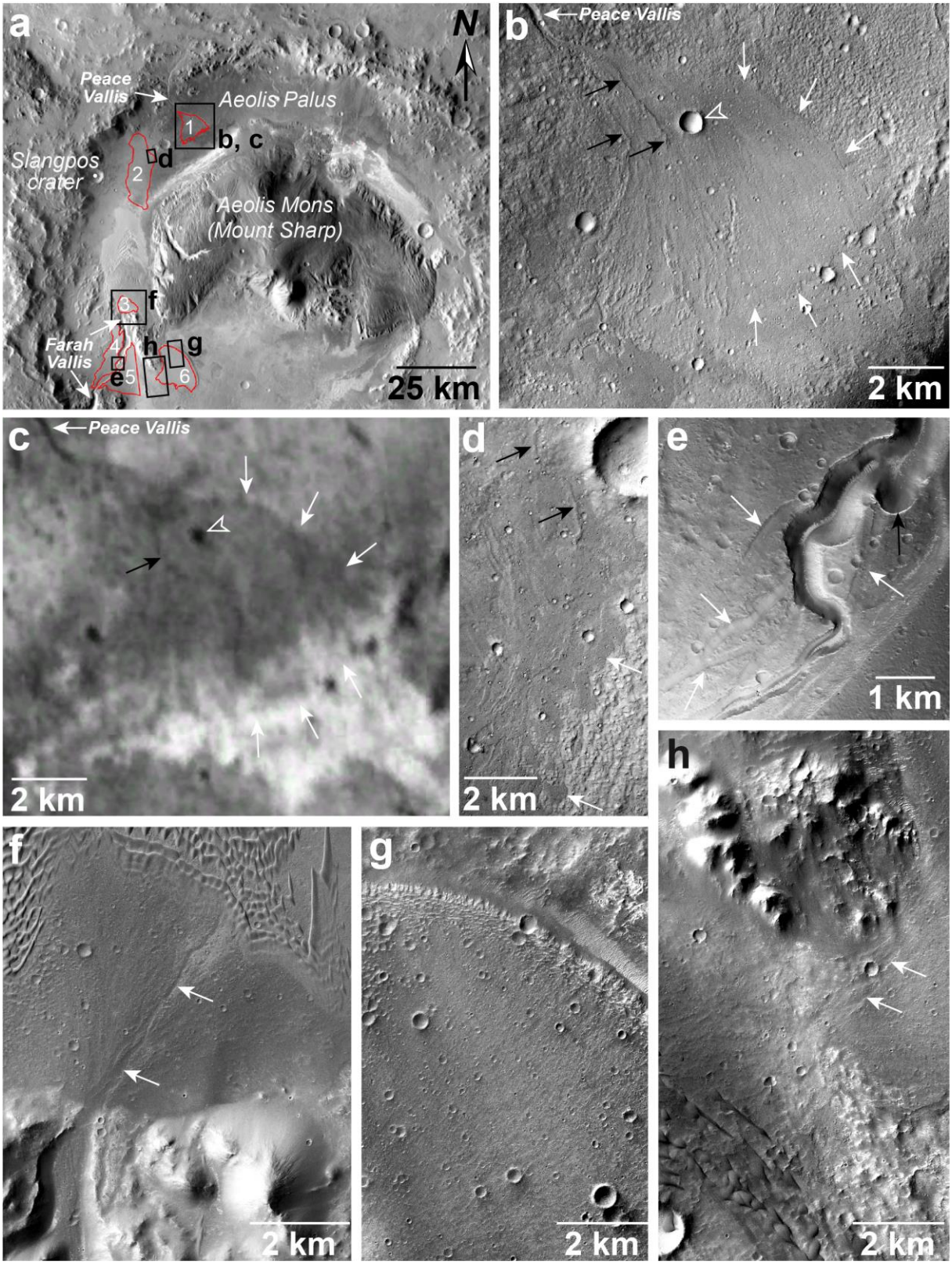

Figure 1. a) Alluvial fans in Gale crater (outlined in red, after Grant et al., 2014), located northwest (NW) and southwest (SW) of Aeolis Mons, include: Peace Vallis fan (1), the NW fan

(after Buz et al., 2017) (2), SW floor fan (3), SW upper fan north of Farah Vallis (4), SW upper fan south of Farah Vallis (5), and the SW floor lobe, or the "pancake delta" (6). Subframe of THEMIS day infrared (IR) mosaic (100 m/pixel). Black boxes indicate locations of b-h. **b**) Peace Vallis fan (see Fig, 1a for context) has distinct margins (e.g., white arrows) and inverted channels (black arrows indicate examples) on the fan surface. Late alluvial activity from Peace Vallis buried the ejecta and part of the outer rim of a ~750m-diameter crater (hollow white arrow). Subframe of CTX merged orthophoto mosaic (Calef & Parker, 2016). **c**) Dark-toned channel (e.g., black arrow), diverted around the west side of the ~750 m-diameter crater (white hollow arrow), is evidence for burial of the crater by late stage activity from Peace Vallis (see Figs. 1a and 1b for context). Fan margins (e.g., white arrows, same as in Fig. 1b) are also evident in the thermal data. Subframe of global THEMIS nighttime IR mosaic (100 m/pixel). **d**) Relatively dark-toned surface of the NW fan (see Fig. 1a for context) exhibits inverted channels (e.g., black arrows) and distinct margins (e.g., white arrows), and superposes the lighter-toned, Aeolis Palus materials (lower right of image). Subframe of HiRISE ESP_025790_1750 (25 cm/pixel). **e**) Abandoned, shallow channels (e.g., white arrows) and a possible plunge pool (black arrow) in Farah Vallis (see Fig. 1a for context). Subframe of HiRISE ESP_033148_1780 (50 cm/pixel). **f**) Main distributary channel(s) (e.g., white arrows) incise the surface of the SW floor fan (see Fig. 1a for context). Subframe of CTX F21_043816_1748 (5.47 m/pixel). **g**) Surface of SW floor fan ("pancake delta," Palucis et al., 2016). Subframe of CTX F21_043816_1748 (5.47 m/pixel). **h**) Faint distributaries (e.g., white arrows) feeding the SW floor lobe or "pancake delta." Subframe of CTX F21_043816_1748 (5.47 m/pixel). North is toward the top in all images.

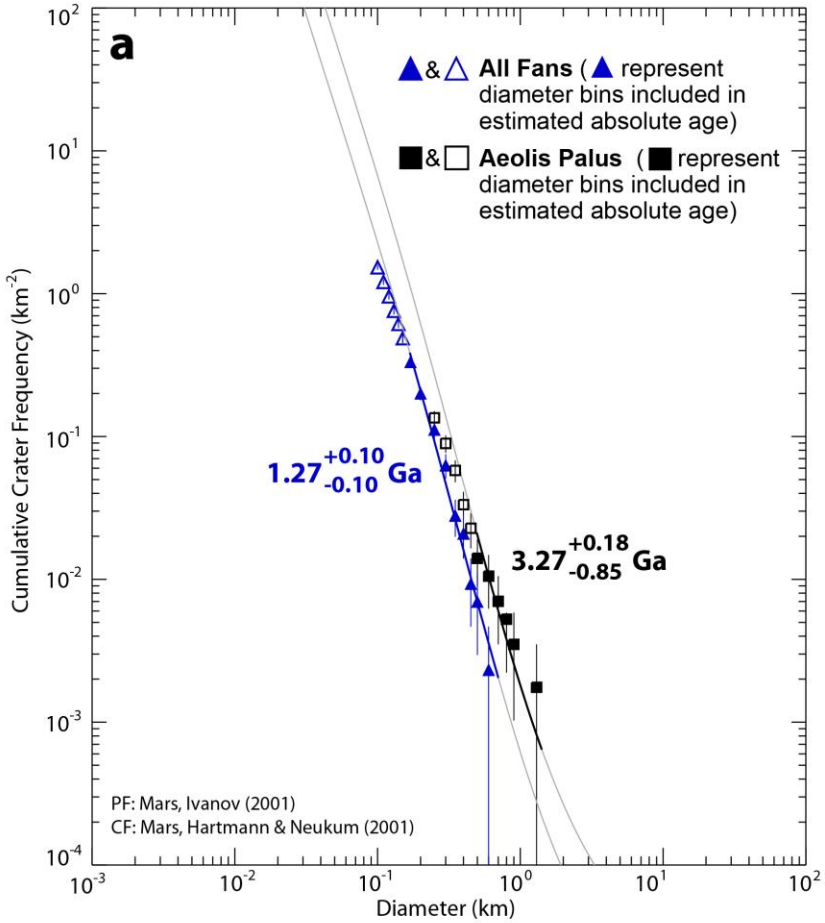
a
▲&△ All Fans (▲ represent diameter bins included in estimated absolute age)
■&□ Aeolis Palus (■ represent diameter bins included in estimated absolute age)
1.27 +0.10 -0.10 Ga
3.27 +0.18 -0.85 Ga
PF: Mars, Ivanov (2001)
CF: Mars, Hartmann & Neukum (2001)
Cumulative Crater Frequency (km-2)
Diameter (km)

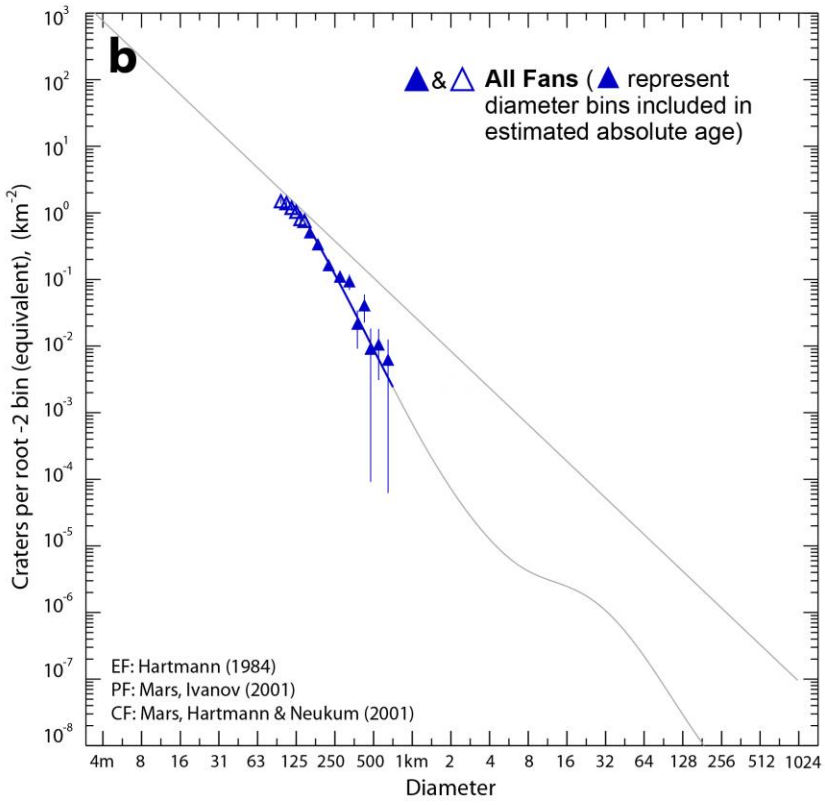
b
▲&△ All Fans (▲ represent diameter bins included in estimated absolute age)
EF: Hartmann (1984)
PF: Mars, Ivanov (2001)
CF: Mars, Hartmann & Neukum (2001)
Craters per root -2 bin (equivalent), (km-2)
4m 8 16 31 63 125 250 500 1km 2 4 8 16 32 64 128 256 512 1024
Diameter

Figure 2. a) Cumulative crater statistics of all of the combined fan surfaces (see Fig. S1) examined in Gale crater (filled and hollow triangles) and Aeolis Palus (filled and hollow squares). The interpreted absolute age of the combined fan areas in Gale of ~1.27 (±0.10) Ga is based on 143 craters in a diameter range from 0.17 to 0.667 km (e.g., filled triangles). N(1) =6.17 x 10^{-4}. Craters ≥ 100 m included in plot (smaller crater diameter bins removed). All fans (N=3,266 craters, A=429 km^2, with individual fan areas of 49 km^2, 90 km^2, 179 km^2, and 111 km^2 for the Peace Vallis fan, NW fan, Farah Vallis fans, and the "pancake delta," respectively). Cumulative crater statistics estimate an age of 3.27 (+0.18/-0.85) Ga based on 8 craters in a diameter range of 0.5 to 1.4 km (e.g., filled squares) for Aeolis Palus (combined area of AP1, AP2 based on Grant et al. (2014) is 570 km^2). N(1)=1.81 x 10^{-3}. Craters > 250 m included in plot (smaller crater diameter bins removed). Production Function (PF) from *Ivanov* (2001); Chronology Function (CF) from Hartmann & Neukum (2001). **b**) The incremental plot suggests an excess of craters in several of the larger diameter bins relative to the cumulative plot, though an interpreted age of 1.3 Ga for the fans in Gale is reasonable. Interpreting the age using 13 craters larger than 350 m diameter yields an age of 1.6 Ga and may be a better fit in the incremental plot, but we use the younger age derived from using the larger number of craters (e.g., filled triangles). Craters ≥ ~ 100 m included in plot (smaller crater diameter bins removed). PF from Ivanov (2001); CF from Hartmann & Neukum (2001), Equilibrium Function (EF) from Hartmann (1984). Error bars reflect +/- $1/N^{0.5}$ and N +/-$N^{0.5}$/A for data in cumulative and incremental plots, respectively (N= number of craters; A=area).